

Delay Spread and Electromagnetic Reverberation in Subway Tunnels and Stations

Lei Zhang, Cesar Briso, Jean Raphaël Olivier Fernandez,
José I. Alonso, Carlos Rodríguez, Juan Moreno García-Loygorri, and Ke Guan

Abstract—This paper presents an extensive campaign of wideband propagation measurements conducted in a modern subway environment in Madrid at 980 MHz and 2450 MHz. Measurements have been made using a channel sounder in a realistic environment of tunnel and station. Based on the measurement results, the principal parameters, such as mean power and delay spread, have been extracted for wideband propagation modelling. Furthermore, the results have been used to model electromagnetic reverberation, quality factor and transition region between tunnel and station. The quantitative results provide a detailed wideband model of subway environment, as well as determine the design trade-offs inside real tunnels and stations, in terms of optimal frequency band, antenna position and expected multipath.

Index Terms—Channel sounding & modelling, delay spread, electromagnetic reverberation, multipath propagation, subway, tunnel.

I. INTRODUCTION

THE DEPLOYMENT of wideband communication systems in railway environment is particularly complex in the subway, where most of the time the train travels through tunnels interspersed with various stations. The research on wideband propagation in subway environment has begun over the last few years, some experimental studies within mainly focused on the propagation in tunnels [1] [2] [3]. These tests suggest that multipath effect is weak in tunnels, and increases in stations where there are dense diffuse multipath components due to the intensive use of steel panels. Therefore, a degradation on the performance of the wideband systems has been reported in [4] [5] [6] in these scenarios. Nevertheless, the propagation has not been modelled in high-multipath regions like the subway stations, and the transition regions between tunnels and stations. For this purpose, room electromagnetic theory [7] can be very useful to understand radio propagation in high-multipath environment [8] [9]. However, to the best of our knowledge, this theory has never been applied to model the wideband propagation in a realistic subway environment of tunnels and stations. Therefore, this paper focuses on

This work was developed under the framework of INNPACTO TECRAIL research project IPT-2011-1034-37000 funded by the Spanish Ministry of Economy and Competitiveness, and supported by the grant FPU12/04139. Financial support of the China Scholarship Council (CSC) research fellowship given to Lei Zhang is also acknowledged.

L. Zhang, C. Briso and J. R. Fernandez are with the ETSIS Telecommunication, and J. I. Alonso is with the ETSI Telecommunication, Technical University of Madrid, Madrid, Spain (e-mail: zlbadiang@gmail.com; cesar.briso@upm.es).

C. Rodríguez and J. M. García-Loygorri are with the Metro de Madrid, S.A. Madrid, Spain.

K. Guan is with the State Key Laboratory of Rail Traffic Control and Safety, Beijing Jiaotong University, Beijing, China.

the analysis of wideband propagation at two typical communications frequencies in a realistic subway environment. Critical wideband parameters have been extracted for tunnel and station with or without train. Then, the accurate values of reverberation time and Q (quality factor) have been obtained in the transition region between tunnel and station at 980 MHz and 2450 MHz. The variation of these parameters have been noticed to be quite relevant in the section of the tunnel next to the station. This variation defines an important transition region that has been modelled along distance. The results obtained can model the wideband propagation in tunnels and stations at different frequencies, and provide a set of valuable conclusions for the radio planning in subway environment.

II. WIDEBAND MEASUREMENT IN REAL SUBWAY TUNNEL AND STATION

The measurements campaign was carried out in a modern subway station of line 3 in Madrid, and the adjoining tunnels. Fig. 1 depicts the main dimensions and shapes of the test environment, where the station is roughly regarded as an “inverted T-shaped” block with 112m long, with a maximum height of 18.47m in the middle. The tunnels have semicircular sections with a 4.17m radius, and have been built with TBM (tunneling boring machine). The train used is the CAF S/3000 type with a length of 89.38m.

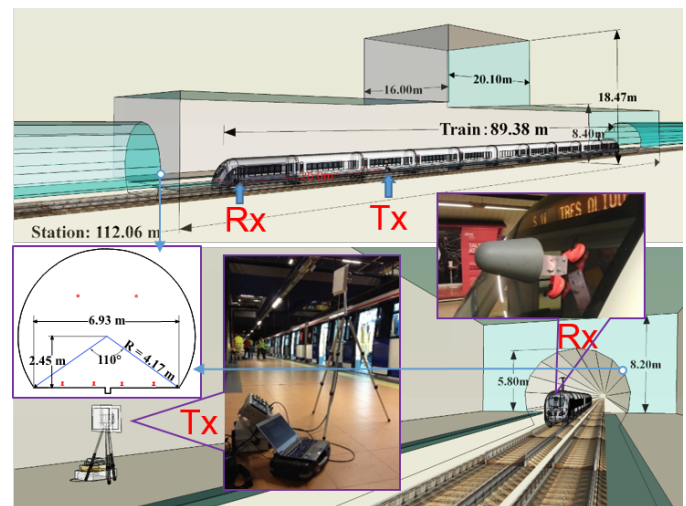


Fig. 1: 3D Models and photos of the measurement scenarios.

The measurements have been made by using a highly portable and configurable channel sounder testbed specially

developed for railway environment [10]. The channel sounder uses the narrow pulse technique to capture the impulse responses of the channel.

The whole measurements are divided into two groups of tests:

- TEST I is designed to model propagation in the station and evaluate the influence of the moving train. During this test, both transmitter and receiver are placed on the platform of the station and separated 20m, as illustrated on the upper part of Fig. 1. In this case, the train is driven on the track near to the channel sounder, and stopped on different positions inside the tunnel and station.
- TEST II is assigned to measure the impulse responses of the channel when the train is passing from the train station into the tunnel. The transmitter is installed in the middle of the station. The receiver is placed in the cabin of the train, with the antenna fixed on the windshield of the rear car. Through this setup, the multipath in the transition region between the tunnel and the station can be recorded.

Both tests have been carried out at 980 MHz and 2450 MHz in a stationary channel with the train stopped and averaging 256 PDPs (Power Delay Profiles) on every position. Detailed configurations and parameters used can be found in TABLE I.

TABLE I: Channel sounder configurations and parameters.

Item	Description
Frequency	980 - 5700 MHz
IF bandwidth	100 MHz
Modulation	Pulse
Pulse width / period	47 / 1500 ns
Tx power	42 dBm
Tx ANT's / g	
Rx ANT (T1) / g	[Patch] HG 908P/8 dBi & 2414P/14 dBi
Rx ANT (T2) / g	[Log-periodic] R&S HL025 / 8 dBi
ANT height	Tx /Rx (T1) /Rx (T2): 2.0m /2.0m /2.2m
Noise figure	4 dB
Demodulation	Logarithmic detector
Sensitivity	- 90 dBm

ANT: antenna; g: gain; T1 / T2: TEST I / TEST II.

III. EXPERIMENTAL RESULTS

In the subway environment, there can be important difference between propagation in tunnels and stations. This section presents the results of the two tests and the parameters extracted by processing the measured delay profile.

A. TEST I: Delay spread in the station.

The main objective of TEST I is to observe the influence of the wall materials (mainly steel), the size of the station, and the impact of a train arriving. For these purposes, the transmitter and receiver are fixed inside the station and the test train is docked on different locations. The PDPs for two locations of the test train are shown in Fig. 2 and Fig. 3, at 980 MHz and 2450 MHz, respectively.

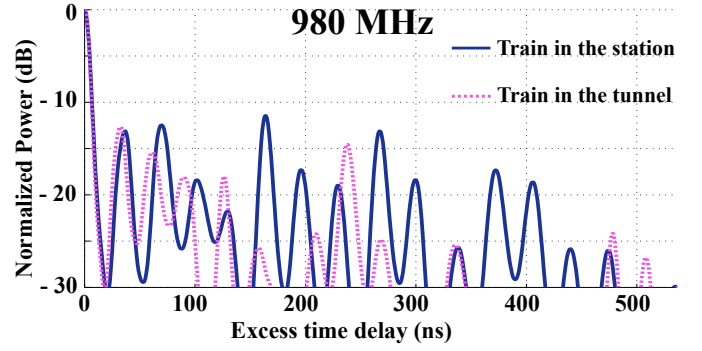


Fig. 2: Two PDP samples in TEST I at 980 MHz.

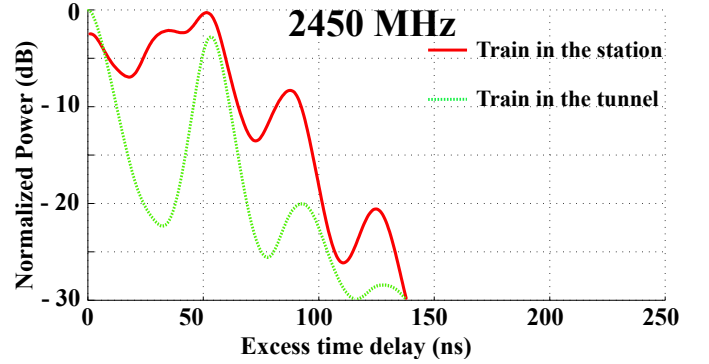


Fig. 3: Two PDP samples in TEST I at 2450 MHz.

The post-processing on PDPs derives the mean of received power, and the RMS (root mean square) delay spread (RMS-DS), which are key parameters to characterize a frequency selective fading.

Eq. (1) expounds the calculation of RMS-DS σ_τ [11], the channel capacities can be compared in terms of this value. Moreover, the statistical results from the collected PDPs in TEST I are presented in TABLE II.

$$\sigma_\tau = \sqrt{\tau^2 - (\bar{\tau})^2} \quad (1)$$

TABLE II: Statistical results in TEST I.

Frequency	Train's location	Mean Power	RMS-DS
980 MHz	In the station	-22.8 dB	159.3 ns
	In the tunnel	-22.2 dB	141.2 ns
2450 MHz	In the station	-11.1 dB	33.6 ns
	In the tunnel	-18.8 dB	37.0 ns

From TABLE II, it can be found that the performances at two different frequencies are significantly different. The RMS-DS is much longer at 980 MHz than at 2450 MHz, which means the diffuse scattering is much higher at 980 MHz due to the smaller free space propagation loss at lower frequency. Therefore higher frequency yields shorter RMS delay and higher data capacity.

Additionally, the tested parameters under the condition of the train present in the station can be compared with the ones in the case of the train is absence, and easily realize that the train affects very mildly to the received signal with very

close RMS-DS. Thus, the influence of the train is rather small, because it only increases the diffuse scattering.

B. TEST II: Delay spread in the tunnel and station with receiver on board the train.

TEST II is aimed to observe the effects in different regions of the tunnel. To reveal these effects, PDPs of several test points along the tunnel and station are collected at a regular distance, and then normalized and represented in Fig. 4. On this figure, the minimum level is limited to a threshold of -30 dB to clarify the reduction of delay spread, when the train goes inside the tunnel. Results are very relevant, and clearly demonstrate how the received power of multipath signals reduces, when the train passes from the station to the deep tunnel. It is noticeable that the multipath components mainly created in the station are impaired gradually by the filtering effect of the tunnel. This effect defines a transition region, where the multipath components are highly reduced from the entrance of the tunnel to the deep tunnel with most of the high order elements are suppressed. This region is much longer at 980 MHz (720m) than at 2400 MHz (350m).

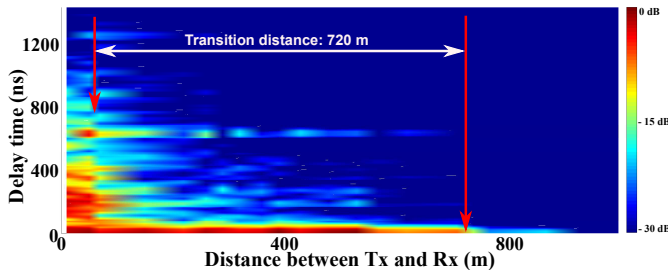


Fig. 4: PDPs variation versus distance at 980 MHz.

In real conditions, subway trains pass continuously from tunnels to stations, hence it is crucial to model the effects of multipath in tunnels and stations, as well as the transition regions. Based on room electromagnetics theory [7], subway environment can be roughly regarded as a lossy cavity. Thus, the reverberation time regards the diffuse absorption gives an idea of the reflection coefficient of the walls in subway station and tunnel, which can be used together with the delay spread to model the channel. Furthermore, the quality factor (Q) can be got based on the reverberation time. The Q value is a more practical parameter that can be used to compare a given environment at different frequencies.

$$\tau_r = \frac{4V}{c_0\eta S} \quad (2)$$

$$Q = 2\pi f\tau_r = Q_{Density} \times K, \text{ where } K = \frac{V}{S}. \quad (3)$$

Eq. (2) and Eq. (3) describe the calculations of the reverberation time and Q factor, where τ_r represents the reverberation time in the reverberation chamber with V volume, c_0 is the velocity of light, and S denotes the area of absorption surface with absorption coefficient η . In our case, the surface of the station is mainly covered by steels. While in the tunnel, inner wall is constructed by the smooth concretes. Based on the

dimensions given in Fig. 1, the K values in tunnel and station are unequal constants, where $K_t \approx 1.8$ in the tunnel and $K_s \approx 2.8$ in the station. Furthermore, based on the derivations in [8] [9], the fitting slope of the decaying part in PDP can be used to obtain the reverberation time as follow:

$$\tau_r = -\frac{10\log(e)}{\text{slope}} \quad (4)$$

Where e is the Eulers constant. If each PDP is imported to Eq. (3) and Eq. (4), one can obtain the variation curves of Q as described in Fig. 5. Therefore, when the reverberation time variation along the distance is obtained through the statistical processing of the measurement results, the $Q_{Density}(d)$ and $\eta(d)$ can be determined as the functions of distance as follows:

$$Q_{Density}(d) = 2\pi f\tau_r(d) \times \frac{1}{K} = \frac{8\pi f}{c_0\eta(d)K} \quad (5)$$

$$\eta(d) = \frac{4K}{c_0\tau_r(d)} \quad (6)$$

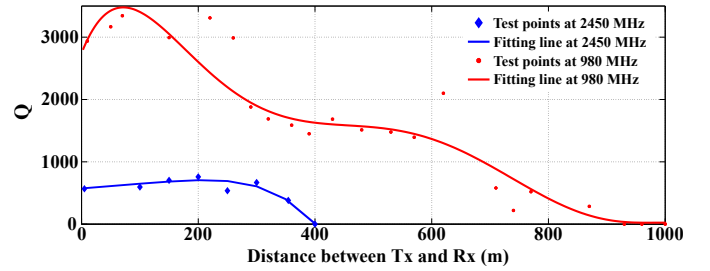


Fig. 5: Q-factor variations versus distance at 980 MHz and 2450 MHz: station from 0 to 50m; tunnel from 50 to 1000m.

As shown in Fig. 5, for 980 MHz, three regions can be clearly defined. *Station* from 0 to 50m, *intermediate tunnel (Inter-Tunnel)* from 50 to 770m and *Deep-Tunnel* over 770m. TABLE III provides the statistical results of TEST II with three regions definitions at two frequencies.

Reverberation time is reduced as the train goes deeper in the tunnel, therefore, Q decreases from high values (3000) in the station to zero after 800m inside the tunnel. The *Station* region has a long reverberation time and a high Q due to the high level of reflections from the walls and pillars covered with steel panels. Later, as the train reaches the *Inter-Tunnel*, there are still many reflected rays propagating inside the tunnel with low attenuation. This phenomenon is much more obvious at 980 MHz than at 2450 MHz, Q factor is smaller and the attenuation of multipath in the tunnel is much faster. Thus, only a transition region of 350m appears over the threshold. Consequently, the *Deep-Tunnel* can be defined as an area with low Q that drastically attenuates multipath components.

Based on the above results, a simplified model is proposed in Fig. 6. The calculation of transition distance D_T is a comprehensive consideration, which is defined by two variables: D_{T1} and D_{T2} as described in Eq. (7). D_{T1} represents the impact of the sizes of the tunnel and station. D_{T2} means the contribution of frequency, which leads the different slopes in D_{T2} .

TABLE III: Statistical results of TEST II.

Frequency	Region	V/S (K)	Distance range	Q_{Avg}	D_T	η_{Avg}	τ_r	RMS-DS
980 MHz	Station	2.8 m	0 - 50 m	3052.6	720 m	0.07	495.7 ns	312.7 ns
	Inter-Tunnel	1.8 m	50 - 770 m	1795.6		0.08	291.6 ns	184.0 ns
	Deep-Tunnel	1.8 m	> 770 m	< 71.3		< 2.1	< 11.6 ns	< 2.6 ns
2450 MHz	Station	2.8 m	0 - 50 m	580.3	350 m	1.0	36.9 ns	22.8 ns
	Inter-Tunnel	1.8 m	50 - 400 m	520.4		1.1	33.8 ns	7.6 ns
	Deep-Tunnel	1.8 m	> 400 m	≈ 0		—	≈ 0 ns	≈ 0 ns

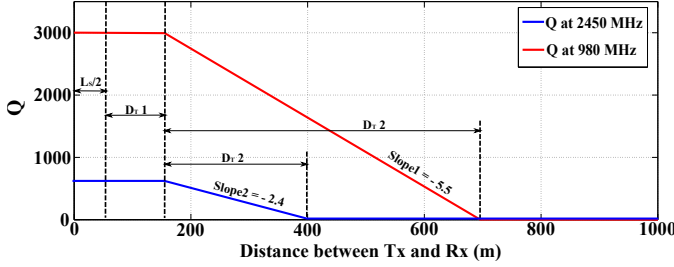


Fig. 6: Transition model based on the Q-factor variations at 980 MHz and 2450 MHz.

$$D_T = D_{T1} + D_{T2} = \frac{L_s K_s}{2K_t} + \frac{Q_s}{-s_0} \times \frac{f}{f_0} \quad (7)$$

$$\approx \left(\frac{L_s}{2K_t} + \frac{8\pi f^2}{5.6 \times c_0 \eta_s} \right) \times K_s$$

Here L_s is the length of the station with absorption coefficient η_s . s_0 and f_0 denote the reference slope and frequency, respectively. Q_s , K_s and L_s represent the corresponding values can be measured in the station. Then, $s_0 \times f_0$ at two frequencies are close to -5.6. The transition distance can be roughly estimated by Eq. (7), when the parameters of station and cross section dimensions are supplied.

Integrating the model with the measurements can provide detailed information about the behavior of wideband communications in subway tunnels and stations, which is useful to chose the optimal antenna configuration and location. Nowadays, most of subway antennas are usually installed in the stations, nevertheless installing them inside the tunnels (after D_{T1}) highly reduces the multipath components. Additionally, if we consider a 2×2 MIMO (Multi-input Multi-output) system in subway tunnel, the channel matrix is singular with a very high condition number caused by the waveguide effect, which means a non-optimal scenario for spatial multiplexing. On the other hand, the condition number is close to 1 in a large station, therefore the spatial multiplexing is applicable, and a MIMO system is helpful in improving the channel capacity.

IV. CONCLUSION

In this paper, a set of wideband communication measurements in a modern and realistic subway environment of tunnel and station have been presented. The RMS-DS and reverberation time extracted from the results are combined to achieve a detailed channel model. The subway station covered with steel panels has shown to be a dense multipath environment, with

long reverberation time and clear differences with the tunnels. Propagations at 2450 MHz have shown to have much less multipath components than at 980 MHz. Also, the movement of the train in the station has small influence on the delay spread. On the other hand, the transition region between tunnel and station has been defined and modelled. In this region, multipath components are reduced by the filtering effect of the tunnel. The region becomes very long at 980 MHz over 720m, while at 2450 MHz it reaches only 350m. In summary, the use of 2.4 GHz or higher frequencies and the location of antennas inside tunnel sections next to the stations, can considerably reduce the multipath effects in subway environment. Future work will be to make a more detailed channel model including the antenna radiation pattern and phase information.

REFERENCES

- [1] J. Alonso, S. Capdevila, B. Izquierdo and J. Romeu, "Propagation Measurements and Simulations in Tunnel Environment at 5.8 GHz," in *Proc. IEEE Int. Symp. Antennas Propag. Soc.*, 2008, pp. 472-475.
- [2] J. Molina-Garcia-Pardo, J.-V. Rodriguez and L. Juan-Llaser, "Wide-band measurements and characterization at 2.1 GHz while entering in a small tunnel," *IEEE Trans. Veh. Technol.*, vol. 53, no. 6, pp. 1794-1799, 2004.
- [3] Y. P. Zhang, G. X. Zheng and J. H. Sheng, "Ray-optical prediction of radio-wave propagation characteristics in tunnel environments. 2. Analysis and measurements," *IEEE Trans. Antennas Propag.*, vol. 46, no. 9, pp. 1337-1345, 1998.
- [4] J. A. Valdesuerio, B. Izquierdo and J. Romeu, "On 2×2 MIMO Observable Capacity in Subway Tunnels at C-Band: An Experimental Approach," *IEEE Antennas Wireless Propag. Lett.*, vol. 9, pp. 1099-1102, 2010.
- [5] C. Sanchis-Borras, J.-M. Molina-Garcia-Pardo, M. Lienard and P. Degauque, "Performance Evaluation of MIMO-OFDM in Tunnels," *IEEE Antennas Wireless Propag. Lett.*, vol. 11, pp. 301-304, 2012.
- [6] J. Moreno, L. de Haro, C. Rodriguez, L. Cuellar, and J. M. Riera, "Key-hole Estimation of an MIMO-OFDM Train-to-Wayside Communication System on Subway Tunnels," *IEEE Antennas Wireless Propag. Lett.*, vol. 14, pp. 88-91, 2015.
- [7] J. B. Andersen, J. O. Nielsen, G. F. Pedersen, G. Bauch, and M. Herdin, "Room Electromagnetics," *IEEE Antennas Propag. Mag.*, vol. 49, no. 2, pp. 27-33, 2007.
- [8] A. Bamba, M. Martinez-Ingles, D. Gaillot, E. Tanghe, B. Hanssens, J. Molina-Garcia-Pardo, and W. Joseph, "Experimental Investigation of Electromagnetic Reverberation Characteristics as a function of UWB Frequencies," *IEEE Antennas Wireless Propag. Lett.*, vol. PP, no. 99, pp. 1-1, 2014.
- [9] J. B. Andersen, K. L. Chee, M. Jacob, G.F. Pedersen, and T. Kurner, "Reverberation and Absorption in an Aircraft Cabin With the Impact of Passengers," *IEEE Trans. Antennas Propag.*, vol. 60, no. 5, pp. 2472-2480, 2012.
- [10] L. Zhang, C. Briso-Rodriguez, J.R.O. Fernandez, and K. Guan, "Channel Sounder and Broadband Measurements for Railway Systems," *IEICE Info. Comm. Technol. Forum (ICTF)*, 2014, COMM2-4.
- [11] L. Liu, T. Chen, J. H. Qiu, H. J. Chen, L. Yu, W. H. Dong, and Y. Yuan, "Position-based modeling for wireless channel on high-speed railway under a viaduct at 2.35 GHz," *IEEE J. Sel. Area. Comm.*, vol. 30, no. 4, pp. 834-845, 2012.